AIP | APL Materials

The impact of sodium contamination in tin sulfide thin-film solar cells

Vera Steinmann, Riley E. Brandt, Rupak Chakraborty, R. Jaramillo, Matthew Young, Benjamin K. Ofori-Okai, Chuanxi Yang, Alex Polizzotti, Keith A. Nelson, Roy G. Gordon, and Tonio Buonassisi

Citation: APL Mater. **4**, 026103 (2016); doi: 10.1063/1.4941713
View online: http://dx.doi.org/10.1063/1.4941713
View Table of Contents: http://scitation.aip.org/content/aip/journal/aplmater/4/2?ver=pdfcov
Published by the AIP Publishing

Articles you may be interested in

Framework to predict optimal buffer layer pairing for thin film solar cell absorbers: A case study for tin sulfide/zinc oxysulfide
J. Appl. Phys. **118**, 115102 (2015); 10.1063/1.4930581

Non-monotonic effect of growth temperature on carrier collection in SnS solar cells
Appl. Phys. Lett. **106**, 203901 (2015); 10.1063/1.4921326

Employing time-resolved terahertz spectroscopy to analyze carrier dynamics in thin-film Cu2ZnSn(S,Se)4 absorber layers
Appl. Phys. Lett. **104**, 253901 (2014); 10.1063/1.4884817

Enhanced omni-directional performance of copper zinc tin sulfide thin film solar cell by gradient index coating
Appl. Phys. Lett. **104**, 101104 (2014); 10.1063/1.4868104

Erratum: “Effects of sodium incorporation in Co-evaporated Cu2ZnSnSe4 thin-film solar cells” [Appl. Phys. Lett. 102, 163905 (2013)]
Appl. Phys. Lett. **103**, 029901 (2013); 10.1063/1.4813746

Reuse of AIP Publishing content is subject to the terms at: https://publishing.aip.org/authors/rights-and-permissions. IP: 128.103.93.158 On: Mon, 29 Feb 2016 20:15:10

The impact of sodium contamination in tin sulfide thin-film solar cells

Vera Steinmann,[1,a] Riley E. Brandt,[1] Rupak Chakraborty,[1] R. Jaramillo,[1] Matthew Young,[2] Benjamin K. Ofori-Okai,[1] Chuanxi Yang,[3] Alex Polizzotti,[1] Keith A. Nelson,[1] Roy G. Gordon,[3] and Tonio Buonassisi[1]
[1]*Massachusetts Institute of Technology, Cambridge, Massachusetts 02139, USA*
[2]*National Renewable Energy Laboratory, Golden, Colorado 80401, USA*
[3]*Department of Chemistry and Chemical Biology, Harvard University, Cambridge, Massachusetts 02138, USA*

(Received 8 December 2015; accepted 28 January 2016; published online 12 February 2016)

Through empirical observations, sodium (Na) has been identified as a benign contaminant in some thin-film solar cells. Here, we intentionally contaminate thermally evaporated tin sulfide (SnS) thin-films with sodium and measure the SnS absorber properties and solar cell characteristics. The carrier concentration increases from 2×10^{16} cm^{-3} to 4.3×10^{17} cm^{-3} in Na-doped SnS thin-films, when using a 13 nm NaCl seed layer, which is detrimental for SnS photovoltaic applications but could make Na-doped SnS an attractive candidate in thermoelectrics. The observed trend in carrier concentration is in good agreement with density functional theory calculations, which predict an acceptor-type Na_{Sn} defect with low formation energy. © *2016 Author(s). All article content, except where otherwise noted, is licensed under a Creative Commons Attribution (CC BY) license (http://creativecommons.org/licenses/by/4.0/).* [http://dx.doi.org/10.1063/1.4941713]

Thin-film photovoltaic (PV) technologies have the potential to become cost-effective alternatives to silicon PV.[1,2] Despite decades of research, only a small number of Earth-abundant thin-film technologies have exceeded 5% laboratory efficiencies to date.[3] Many of the new-emerging polycrystalline thin-film absorbers suffer from high recombination losses in the bulk and at grain boundaries.

Major device efficiency improvements have been empirically observed in some inorganic thin-film technologies (e.g., CdTe,[4–6] $CuIn_xGa_{(1-x)}Se_2$,[7–9] and Cu_2ZnSnS_4[10–12]) when contaminated with alkali metals. Those additives were found to stimulate grain growth in polycrystalline films and passivate grain boundaries. In Cu_2ZnSnS_4 solar cells, in particular, sodium (Na) additives were found to enhance grain growth and passivate grain boundaries, reducing charge carrier recombination losses.[12]

In this study, we test the hypothesis that alkali metal additives, specifically sodium following the example of the Cu_2ZnSnS_4 study by Gershon *et al.*, also improve the device performance of tin sulfide (SnS) thin-film solar cells. SnS is considered a promising Earth-abundant PV material because of its high absorption coefficient,[13–15] tunable majority carrier (holes) concentration (10^{15}-10^{18} cm^{-3}),[13,16] high hole mobility,[16,17] and its potential for low-cost manufacturing.[18] In recent years, efficiency improvements from 1.3%[13] to 4.36%[19] have been achieved by engineering the SnS bulk (i.e., grain growth through post-deposition H_2S annealing)[18–20] and the absorber/buffer layer interface (i.e., tuning band offset and carrier concentration in the buffer layer).[21,22] The SnS device performance to date is believed to be predominantly limited by charge-carrier recombination in the absorber bulk. In previous work, relatively short charge-carrier diffusion lengths of ~200 nm were estimated, compared to the SnS film thickness of 1 μm.[17,23]

When comparing the thermally evaporated SnS solar cell characteristics of intentionally Na-doped devices to undoped references devices, no statistically significant difference is observed. We

[a]vsteinma@mit.edu

 © Author(s) 2016.

Reuse of AIP Publishing content is subject to the terms at: https://publishing.aip.org/authors/rights-and-permissions. IP: 128.103.93.158 On: Mon, 29 Feb 2016 20:15:10

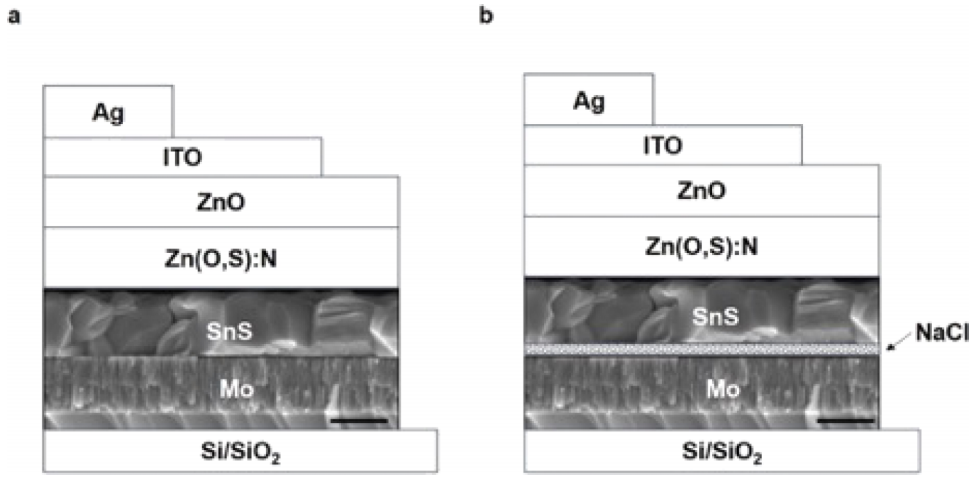

FIG. 1. Cross-sectional schematics of tin sulfide (SnS) solar cell device stacks. (a) Reference SnS device stack as published in Ref. 18. (b) SnS device stack including a thermally evaporated 13 nm NaCl layer between the Mo back contact and the SnS absorber film to achieve Na-doping in the SnS bulk via in-diffusion upon annealing. The contact layers are not drawn to scale. The cross-sectional scanning electron micrograph depicts the molybdenum back contact and the SnS absorber layer in the device stack; the scale bar indicates 500 nm.

verify sodium diffusion into the SnS bulk from an underlying NaCl seed layer via secondary ion mass spectrometry (SIMS). To understand the role of sodium in SnS thin-film solar cells, we study the structural and electronic properties of intentionally Na-doped SnS thin-films in comparison to undoped reference SnS thin-films. We compare our experimental observations to calculations by density functional theory (DFT) on SnS.[24,25] Finally, we perform 1D device simulations using SCAPS (solar cell capacitance simulator)[26] to guide the discussion on the impact of Na contamination in SnS thin-film solar cells.

SnS thin-film solar cells were fabricated following the recipe published in Refs. 18 and 27. For the Na-doped SnS solar cells, we thermally evaporated a thin layer of NaCl (13 ± 2 nm) on top of the molybdenum metal back contact prior to the SnS deposition. The device stacks for the reference SnS device and the Na-doped SnS device are illustrated in Figs. 1(a) and 1(b), respectively.

The solar cells were characterized at room temperature (24.9 °C) by current density-voltage (J-V) and external quantum efficiency (EQE) measurements, using a Keithley 2400 sourcemeter. The standard illumination of 100 mW cm^{-2} was generated by a Newport Oriel 91194 solar simulator with a 1300 W Xe-lamp using an AM1.5G filter, and a Newport Oriel 68951 flux controller was calibrated by a National Renewable Energy Laboratory (NREL)-certified silicon reference cell equipped with a BK-7 window. A shadow mask of 0.25 cm^2 area was used to mask the illuminated area during J-V measurements on SnS devices. The EQE measurements were performed with a PV Measurements Model QEX7 tool.

The sodium content in the reference SnS thin-film and the Na-doped SnS thin-film was measured via SIMS (CAMECA IMS). The morphology of reference SnS thin-films and Na-doped SnS thin-films was imaged by field-emission scanning electron microscopy (FESEM, Zeiss, Ultra-55). The crystal structure and texture of the films were analyzed by X-ray diffraction (XRD, Rigaku SmartLab) with Cu $K\alpha$ radiation using a θ-2θ scan. SIMS, FESEM, and XRD measurements were performed on H_2S annealed SnS thin-films (1 μm thickness) on Si/SiO_2/Mo and Si/SiO_2/Mo/NaCl stacks, respectively.

The majority carrier concentration and mobility were determined from Hall effect measurements. Reference SnS thin-films were fabricated on 8×8 mm^2 insulating Si/SiO_2 substrates. Na-doped SnS thin-films were fabricated using Si/SiO_2 substrates coated with 13 nm of NaCl. Au top contacts were deposited by e-beam evaporation. The minority carrier lifetime was determined from free carrier absorption measurements, using time-resolved optical terahertz (THz) probe spectroscopy.[28] This measurement required the fabrication of SnS thin-films on transparent quartz substrates. Na-doped SnS thin-films were fabricated by depositing a 13 nm thin NaCl layer prior to

Reuse of AIP Publishing content is subject to the terms at: https://publishing.aip.org/authors/rights-and-permissions. IP: 128.103.93.158 On: Mon, 29 Feb 2016 20:15:10

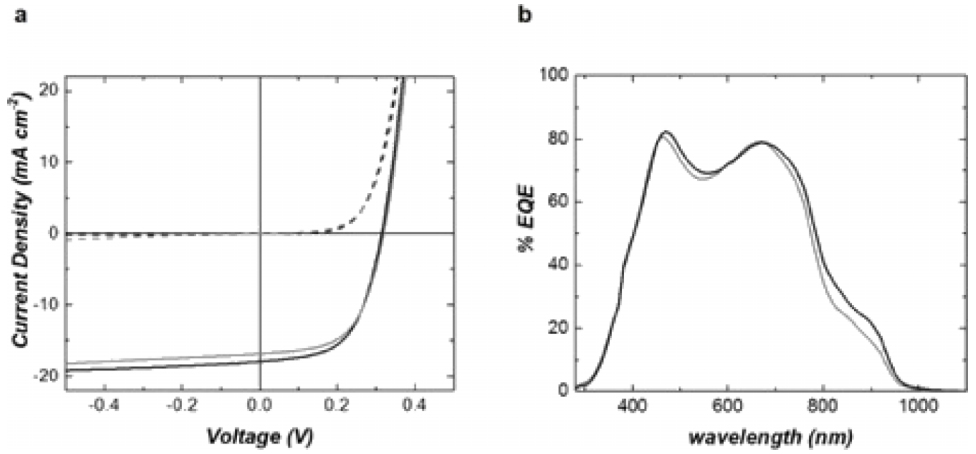

FIG. 2. (a) Current density – voltage (J-V) characteristics and (b) external quantum efficiency (EQE) data of a representative SnS reference device (grey line) and a representative Na-doped SnS device. A small increase in current density (5% relative) is observed upon Na-doping which is in agreement with the slightly increased EQE signal at higher wavelengths (800–900 nm).

the SnS deposition. All specialized reference and Na-doped SnS thin-film samples were fabricated as "sister" samples to the reference and Na-doped device samples, meaning that all reference SnS samples and all Na-doped SnS samples were batch-processed, being exposed to the same SnS deposition and H_2S annealing treatment.

In Fig. 2, the J-V and EQE data of a representative SnS reference thin-film solar cell (grey lines) and a representative Na-doped SnS device (black lines) are compared. The solar cell characteristics of both devices appear to be very similar, suggesting that the intentional Na-doping has little to almost no effect on the overall device performance. We observe a small reduction in the leakage current density in the dark (see dashed lines) and a small increase in the mean short-circuit current density (J_{SC}) under illumination (see solid lines) for the Na-doped device. We attribute the leakage current to shunting in the SnS thin-film devices which is caused by through-thickness voids in the SnS absorber layer. The observed small difference in J_{SC} is in agreement with the observed EQE response. The Na-doped device yields an enhanced EQE response at longer wavelengths (800–950 nm), which could be attributed to enhanced long-wavelength absorption or improved charge-carrier collection. UV-Vis data may suggest a slight (1.1×) increase in long-wavelength absorption (between 850 and 900 nm) in Na-doped SnS samples. However, this change in absorption is within the experimental error. Further, reflectivity data indicate no difference in reflectance between Na-doped SnS and SnS reference devices in the long-wavelength range (800-900 nm). The mean values for the Na-doped and the undoped reference devices are statistically indistinguishable within a 95% confidence interval, when taking into account the spread in solar cell performance across ten individually measured devices.

To check whether sodium has diffused into the SnS bulk upon H_2S annealing, we perform SIMS measurements on a representative SnS reference thin-film and a representative Na-doped SnS thin-film, respectively. Fig. 3 reveals the SIMS data on both samples, verifying that sodium has diffused from the NaCl seed layer into the SnS bulk. As Na ionizes more readily than S or Sn, its signal intensity is not a direct measure of concentration, but can be compared between the two different samples. Note that we also detect sodium in the reference SnS thin-film (Figure 3(a)). The intentionally Na-doped SnS thin-film has a factor of 36 greater sodium concentration than the reference film. In both samples, sodium appears to be evenly distributed in the SnS bulk (0.1–0.8 μm depth, see Figure 3). However, a significantly higher sodium density (~1000×) is detected near the back contact (0.8–0.9 μm depth, see Fig. 3). This suggests that not all sodium atoms have diffused from the NaCl seed layer into the SnS bulk, but instead have formed clusters or small crystallites near the back contact. Note that we cannot make any statements regarding chlorine remnants in

Reuse of AIP Publishing content is subject to the terms at: https://publishing.aip.org/authors/rights-and-permissions. IP: 128.103.93.158 On: Mon, 29 Feb 2016 20:15:10

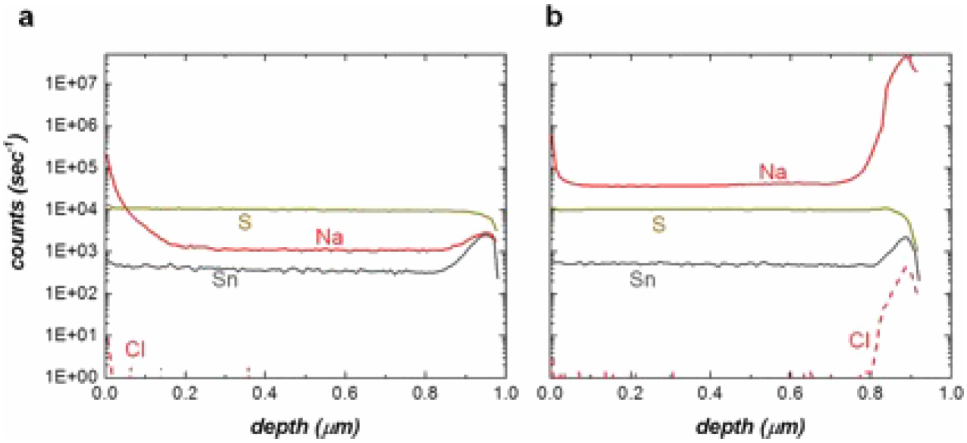

FIG. 3. Secondary ion mass spectrometry (SIMS) data, confirming the penetration of sodium into the SnS bulk. The sodium counts (red solid traces) are more than an order of magnitude higher in the (b) Na-doped SnS thin-film compared to the (a) reference SnS thin-film. The SnS bulk thickness is 1 μm. The sulfur (dark yellow traces) and tin (dark grey traces) are similar in both samples (a) and (b). The dashed red line shows the chlorine signal. Note that chlorine is charged negatively and therefore has a lower ionization probability and higher detection limit in these samples. Signal intensities do not indicate absolute concentrations; Na and S ionize more readily and thus appear with stronger signals than Sn.

the Na-doped SnS thin-film sample because the positively charged primary ion beam is unlikely to ionize the negatively charged Cl^-.

From these SIMS measurements, we conclude that additional sodium is present in the intentionally doped SnS solar cell. Still, no statistically significant impact of sodium additives on the overall device performance is observed. We hypothesize that the excess sodium may cause several counterbalancing effects on absorption and/or charge transport characteristics. In the following, we investigate the structural and electronic properties of reference SnS thin-films and Na-doped SnS thin-films to analyze the impact of sodium contamination on the SnS absorption and charge transport characteristics.

We first consider structural changes in the Na-doped SnS thin-film, which may affect the absorption characteristics. We study the morphology and structure of annealed SnS thin-films with and without Na-doping, using scanning electron microscopy (SEM) and XRD. Fig. 4 reveals SEM plan-view and cross section images as well as the XRD patterns of a representative reference SnS thin-film and a representative Na-doped SnS thin-film, respectively. The SEM images indicate no morphological changes when adding sodium into the SnS thin-film. No large NaCl clusters are observed in the SnS bulk or at the Mo back contact. We further observe in XRD that the Na-doping reveals no impact on the preferred SnS grain orientation. Hence, we find no evidence of structural changes in the Na-doped SnS absorber layer, which would affect the SnS absorption characteristics.

We then consider possible changes in the electronic properties, affecting charge collection in the Na-doped SnS device. Previous SnS device studies indicate that the J_{SC} of the reference SnS device is predominantly limited by recombination losses in the absorber bulk.[18,22,23,28] Changes in the charge carrier mobility-lifetime product may be directly reflected in the J_{SC} measurement.

We measure the majority carrier (hole) concentration and mobility via Hall effect measurements, as well as the minority carrier (electron) lifetime via free carrier absorption measurements for SnS thin-films with and without intentional Na-doping. The results are displayed in Table I.

We observe an increase in majority carrier concentration in the Na-doped sample. This is in good agreement with DFT calculations by Malone *et al.*[25] which predict sodium to form an acceptor-type Na_{Sn} defect (i.e., p-type dopants) at low formation energy in SnS. Note that the tin atoms in SnS are present in the Sn^{2+} state. This is in contrast to, e.g., $CuIn_xGa_{(1-x)}Se_2$ and Cu_2ZnSnS_4, where sodium is assumed to form cation-antisite defects.[29,30] Hall effect measurements indicate an increase in hole concentration by a factor of 20 and a decrease in hole mobility by a factor of 5 in the SnS thin-film with increased sodium concentration. Free carrier absorption measurements suggest minority carrier lifetimes of 38 ps and 21 ps in the undoped and Na-doped

Reuse of AIP Publishing content is subject to the terms at: https://publishing.aip.org/authors/rights-and-permissions. IP: 128.103.93.158 On: Mon, 29 Feb 2016 20:15:10

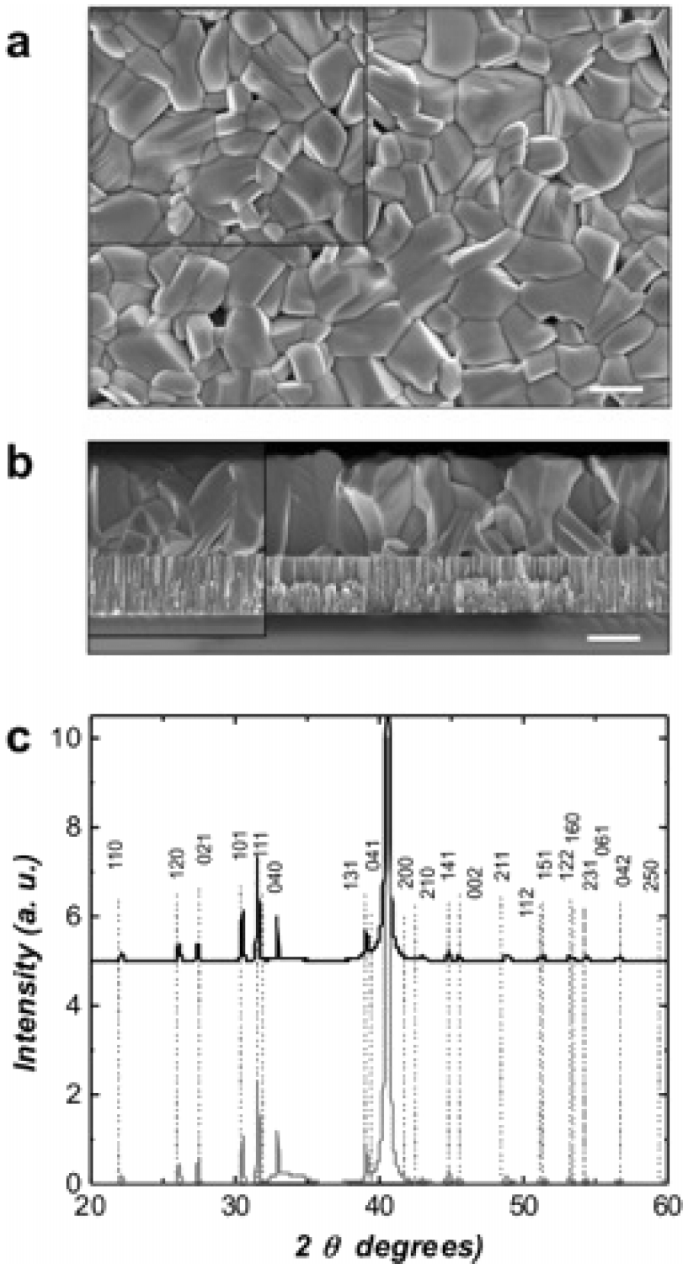

FIG. 4. (a) plan-view and (b) cross-sectional scanning electron microscopy (SEM) images comparing the morphology of a representative SnS reference thin-film (insets) and a representative Na-doped SnS thin-film (large images) reveals no morphological changes upon Na-doping. The scale bar indicates 500 nm. (c) X-ray diffraction (XRD) data normalized to the (111) peak indicates no change in preferred orientation when comparing a representative SnS reference thin-film (grey line) and a representative Na-doped SnS thin-film, both grown on a molybdenum back contact. Both films are phase-pure (JCPDS No. 00-39-0354). Note that the large peak at 40.5 degrees results from the molybdenum back contact. The broad response peak around 33–34 degrees results from the underlying Si substrate.

SnS thin-films, respectively. However, the device efficiency is not expected to strongly correlate with the minority carrier lifetime when the absolute change in lifetime is that small.[28]

We conclude that the obtained results from Hall effect measurements cannot explain the observed trend in device performance. Device simulations would suggest that a decrease in charge carrier mobility results in a decrease in J_{SC} as well. While we do not have a direct measure of the electron mobility, a possible correlation between the hole and electron mobility can be made

Reuse of AIP Publishing content is subject to the terms at: https://publishing.aip.org/authors/rights-and-permissions. IP: 128.103.93.158 On: Mon, 29 Feb 2016 20:15:10

TABLE I. Hole concentration p and mobility μ_h are determined from Hall effect measurements in the reference SnS thin-film and the Na-doped SnS thin-film, respectively. The minority carrier lifetime τ_e is determined from free carrier absorption measurements.[28] Note that the Hall measurements were performed on insulating Si/SiO_2 substrates, whereas the free carrier absorption measurements required the use of transparent quartz substrates. The influence of the underlying substrate on the SnS bulk properties has not been subject to this study.

	p ($\times 10^{16}$ cm^{-3})	μ_h (cm^2/Vs)	τ_e (ps)
Reference SnS thin-film	2.0 ± 0.5	38 ± 2	38 ± 1
Na-doped SnS thin-film	43.0 ± 3.0	7 ± 1	21 ± 1

through effective masses. Using the measured hole mobility and the effective mass ratio m_h/m_e,[21,22] the electron mobility is estimated to be 94 cm^2/Vs in the reference SnS thin-film and 17 cm^2/Vs in the Na-doped SnS thin-film, respectively.

The present study may help to explain why previous experiments on controlling the intrinsic point-defect density by H_2S annealing did not result in any changes in carrier concentration[31] and suggest that future efforts to control doping in thin-film semiconductors must strongly consider the background impurity concentrations.

The origin of the sodium in the SnS reference sample is still unknown. We synthesize thermally evaporated SnS thin-films from commercially available SnS feedstock of ≥99.99% elemental purity. SnS thin-films are processed following best practices to reduce contamination sources. The presented SIMS scan only accounts for sodium present in the SnS bulk, but these thin-films may contain other potentially lifetime limiting contaminants (e.g., metals), which have not been identified yet. Note that the impact of impurities is well studied in silicon[32–35] and has recently been explored in Cu_2ZnSnS_4.[36] To conduct well controlled contamination studies in SnS, a reference SnS sample of higher purity will be required. We are currently exploring approaches to purify the SnS feedstock and to identify lifetime limiting contaminants in SnS.

In summary, we evaluated the effects of intentionally sodium doping thermally evaporated SnS films during growth. Carrier concentrations are observed to increase by over an order of magnitude, to 4.3×10^{17} cm^{-3}, when using a 13 nm thick NaCl seed layer. In principle, carrier concentrations in the range of 10^{18}–10^{19} cm^{-3} should be attainable as the sodium doping concentration in the SnS bulk is further increased. This could make Na-doped SnS an attractive candidate material for thermoelectric applications. The thermoelectric potential of SnS has been previously addressed in the literature.[37,38]

While comparison with a sodium-free SnS reference is not possible based on the present data, nevertheless, Hall effect and free carrier absorption measurements indicate a change in the SnS thin-film electronic properties with increasing sodium concentration in the SnS bulk. Interestingly, the addition of Na-doping at the levels investigated in this study does not affect the performance of SnS thin-film solar cells appreciably, in contrast to other better-studied chalcogenide material systems.

The authors thank M. L. Castillo for her help with substrate preparation and J. R. Poindexter for fruitful discussions. This work is supported by the U.S. Department of Energy through the SunShot Initiative under Contract No. DE-EE0005329 and the National Science Foundation Grant No. CHE-11115577. V. Steinmann, R. E. Brandt, B. K. Ofori-Okai, A. Polizzotti, R. Chakraborty, and R. Jaramillo acknowledge the support of the Alexander von Humboldt foundation, NSF Fellowships, a MITei TOTAL fellowship, and a DOE EERE Postdoctoral Research Award, respectively. This work made use of the Center for Materials Science and Engineering at MIT which is supported by the National Science Foundation (NSF) under Award No. DMR-08-19762 and the Center for Nanoscale Systems at Harvard University which is supported by NSF under Award No. ECS-0335765.

[1] M. Woodhouse, A. Goodrich, R. Margolis, T. James, R. Dhere, T. Gessert, T. Barnes, R. Eggert, and D. Albin, Sol. Energy Mater. Sol. Cells **115**, 199 (2013).
[2] M. Woodhouse, A. Goodrich, R. Margolis, T. L. James, M. Lokanc, and R. Eggert, "Supply-chain dynamics of tellurium, indium, and gallium within the context of PV module manufacturing costs," IEEE J. Photovoltaics (published online 2012).
[3] V. Steinmann, R. E. Brandt, and T. Buonassisi, Nat. Photonics **9**, 355 (2015).

Reuse of AIP Publishing content is subject to the terms at: https://publishing.aip.org/authors/rights-and-permissions. IP: 128.103.93.158 On: Mon, 29 Feb 2016 20:15:10

[4] S. Lalitha, R. Sathyamoorthy, S. Senthilarasu, and A. Subbarayan, Sol. Energy Mater. Sol. Cells **90**, 694 (2006).
[5] A. Abbas, P. Kaminski, G. West, K. Barth, W. Sampath, J. Bowers, and J. M. Walls, MRS Proc. **1738**, mrsf14-1738-v03-03 (2015).
[6] P. D. Paulson and V. Dutta, Thin Solid Films **370**, 299 (2000).
[7] B. T. L. M. Mansfield, I. L. Repins, S. Glynn, J. W. Pankow, M. R. Young, C. DeHart, R. Sundaramoorthy, and C. L. Beall, in *2011 IEEE 37th Photovoltaic Specialists Conference (PVSC)* (IEEE, 2014), pp. 3636–3641.
[8] P. T. Erslev, J. W. Lee, W. N. Shafarman, and J. D. Cohen, Thin Solid Films **517**, 2277 (2009).
[9] A. Rockett, Thin Solid Films **480-481**, 2 (2005).
[10] W. M. Hlaing, J. L. Johnson, A. Bhatia, E. A. Lund, M. M. Nowell, and M. A. Scarpulla, J. Electron. Mater. **40**, 2214 (2011).
[11] B. T. Gershon, Y. S. Lee, R. Mankad, O. Gunawan, T. Gokmen, D. Bishop, B. McCandless, and S. Guha, Appl. Phys. Lett. **106**, 123905 (2015).
[12] T. Gershon, B. Shin, N. Bojarczuk, M. Hopstaken, D. B. Mitzi, and S. Guha, Adv. Energy Mater. **5**, 1400849 (2015).
[13] K. T. Ramakrishna Reddy, N. Koteswara Reddy, and R. W. Miles, Sol. Energy Mater. Sol. Cells **90**, 3041 (2006).
[14] P. Sinsermsuksakul, J. Heo, W. Noh, A. S. Hock, and R. G. Gordon, Adv. Energy Mater. **1**, 1116 (2011).
[15] K. Hartman, J. L. Johnson, M. I. Bertoni, D. Recht, M. J. Aziz, M. A. Scarpulla, and T. Buonassisi, Thin Solid Films **519**, 7421 (2011).
[16] H. Noguchi, A. Setiyadi, H. Tanamura, T. Nagatomo, and O. Omoto, Sol. Energy Mater. Sol. Cells **35**, 325 (1994).
[17] R. Chakraborty, V. Steinmann, N. M. Mangan, R. E. Brandt, J. R. Poindexter, R. Jaramillo, J. P. Mailoa, K. Hartman, A. Polizzotti, C. Yang, R. G. Gordon, and T. Buonassisi, Appl. Phys. Lett. **106**, 203901 (2015).
[18] V. Steinmann, R. Jaramillo, K. Hartman, R. Chakraborty, R. E. Brandt, J. R. Poindexter, Y. S. Lee, L. Sun, A. Polizzotti, H. H. Park, R. G. Gordon, and T. Buonassisi, Adv. Mater. **26**, 7488 (2014).
[19] P. Sinsermsuksakul, L. Sun, S. W. Lee, H. H. Park, S. B. Kim, C. Yang, and R. G. Gordon, Adv. Energy Mater. **4**, 1400496 (2014).
[20] H. H. Park, R. Heasley, L. Sun, V. Steinmann, R. Jaramillo, K. Hartman, R. Chakraborty, P. Sinsermsuksakul, D. Chua, T. Buonassisi, and R. G. Gordon, Prog. Photovoltaics **23**, 901 (2014).
[21] N. M. Mangan, R. E. Brandt, V. Steinmann, R. Jaramillo, J. V. Li, J. R. Poindexter, K. Hartman, L. Sun, R. G. Gordon, and T. Buonassisi, in *2014 IEEE 40th Photovoltaic Specialists Conference (PVSC)* (IEEE, 2014), pp. 2373–2378.
[22] N. M. Mangan, R. E. Brandt, V. Steinmann, R. Jaramillo, C. Yang, J. R. Poindexter, R. Chakraborty, H. H. Park, X. Zhao, R. G. Gordon, and T. Buonassisi, J. Appl. Phys. **118**, 115102 (2015).
[23] J. R. Poindexter, R. E. Brandt, N. M. Mangan, and T. Buonassisi, MRS Proc. **1771**, 139 (2015).
[24] J. Vidal, S. Lany, M. d'Avezac, A. Zunger, A. Zakutayev, J. Francis, and J. Tate, Appl. Phys. Lett. **100**, 032104 (2012).
[25] B. D. Malone, A. Gali, and E. Kaxiras, Phys. Chem. Chem. Phys. **16**, 26176 (2014).
[26] M. Burgelman, J. Verschraegen, S. Degrave, and P. Nollet, Prog. Photovoltaics **12**, 143 (2004).
[27] R. Jaramillo, V. Steinmann, C. Yang, K. Hartman, R. Chakraborty, J. R. Poindexter, M. L. Castillo, R. Gordon, and T. Buonassisi, J. Visualized Exp. **99**, e52705 (2015).
[28] R. Jaramillo, M.-J. Sher, B. K. Ofori-Okai, V. Steinmann, C. Yang, K. Hartman, K. A. Nelson, A. M. Lindenberg, R. G. Gordon, and T. Buonassisi, J. Appl. Phys. **119**, 035101 (2016).
[29] S. Schuler, S. Siebentritt, S. Nishiwaki, N. Rega, J. Beckmann, S. Brehme, and M. C. Lux-Steiner, Phys. Rev. B **69**, 045210 (2004).
[30] A. Nagaoka, H. Miyake, T. Taniyama, K. Kakimoto, Y. Nose, M. A. Scarpulla, and K. Yoshino, Appl. Phys. Lett. **104**, 152101 (2014).
[31] K. Hartman, "Annealing for intrinsic point-defect control and enhanced solar cell performance: The case of H_2S and tin sulfide (SnS)," Ph.D. thesis, Massachusetts Institute of Technology, 2015.
[32] G. Coletti, R. Kvande, V. D. Mihailetchi, L. J. Geerligs, L. Arnberg, and E. J. Ovrelid, J. Appl. Phys. **104**, 104913 (2008).
[33] D. P. Fenning, A. S. Zuschlag, M. I. Bertoni, B. Lai, G. Hahn, and T. Buonassisi, J. Appl. Phys. **113**, 214504 (2013).
[34] B. Michl, J. Schön, F. Schindler, W. Warta, and M. C. Schubert, in *27th European Photovoltaic Solar Energy Conference and Exhibition* (EU PVSEC Proceedings, 2012), p. 709
[35] M. A. Jensen, J. Hofstetter, A. E. Morishige, G. Coletti, B. Lai, D. P. Fenning, and T. Buonassisi, Appl. Phys. Lett. **106**, 202104 (2015).
[36] A. D. Collord, H. Xin, and H. W. Hillhouse, IEEE J. Photovoltaics **5**, 288 (2015).
[37] D. Parker and D. J. Singh, J. Appl. Phys. **108**, 1 (2010).
[38] Q. Tan, L.-D. Zhao, J.-F. Li, C.-F. Wu, T.-R. Wei, Z.-B. Xing, and M. G. Kanatzidis, J. Mater. Chem. A **2**, 17302 (2014).

Reuse of AIP Publishing content is subject to the terms at: https://publishing.aip.org/authors/rights-and-permissions. IP: 128.103.93.158 On: Mon, 29 Feb 2016 20:15:10